ELSEVIER

Ceramics International 33 (2007) 83–88

CERAMICS INTERNATIONAL

www.elsevier.com/locate/ceramint

Preparation and characterization of forsterite (Mg_2SiO_4) bioceramics

Siyu Ni [a,c], Lee Chou [b], Jiang Chang [a,*]

[a] *Biomaterials and Tissue Engineering Research Center, Shanghai Institute of Ceramics, Chinese Academy of Sciences, 1295 Dingxi Road, Shanghai 200050, China*

[b] *Department of Biomaterials, Goldman School of Dental Medicine, Boston University, Boston, MA 02118, USA*

[c] *Graduate School of Chinese Academy of Science, Shanghai 200050, China*

Received 25 May 2005; received in revised form 25 June 2005; accepted 29 July 2005
Available online 21 September 2005

Abstract

Forsterite (Mg_2SiO_4) ceramics were prepared by sintering the Mg_2SiO_4 green compacts at 1350–1550 °C and the sintering behavior and mechanical properties were examined. The results showed that the optimal bending strength (203 MPa) and fracture toughness (2.4 MPa $m^{1/2}$) of forsterite ceramics were obtained after hot treatment at 1450 °C for 8 h, which were higher than those of the currently available hydroxyapatite ceramics. In order to clarify the biocompatibility of the forsterite ceramics, osteoblast adhesion and proliferation experiments were carried out. Well-spread cells were observed on the surface of forsterite ceramics. In addition, MTT tests confirmed that the osteoblast proliferation rate was significantly higher on the surface of the sintered ceramics than on the controls at 7 days ($p < 0.05$). These findings suggest that forsterite ceramics possess good biocompatibility and mechanical properties and might be suitable for potential application like bone implant material.

Keywords: C. Mechanical properties; Forsterite; Biocompatibility

1. Introduction

During the last decades, a variety of biocompatible graft materials have been used as substitute parts of hard tissue [1–3]. Bioceramics have attracted wide attention due to their cheapness, easy production and good biocompatibility. The development of bioceramics has provided promising alternatives to replacing or increasing parts of the skeletal system [4]. Therefore, it is significant to develop new-type of bioceramics.

In recent years, some Si and Mg containing ceramics have drawn interests in the development of bone implant materials [5–11]. Previous research suggests that silicon, as an essential element in skeletal development. Calrisle [12] first reported in the 1970s that silicon was uniquely localized in the active areas of young bone and involved in the early stage of bone calcification. Similar studies by Schwarz and Milne [13] have shown that silicon deficiency in rats resulted in skull deformation, with the cranial bones appearing flatter than normal. Magnesium is also undoubtedly one of the most important elements in human body, and closely associated with mineralization of calcined tissues [14] and indirectly influences mineral metabolism [15].

Forsterite (Mg_2SiO_4) and enstatite ($MgSiO_3$) are important materials in the magnesia–silica system, which are known to be as insulators at high frequencies [16]. Furthermore, enstatite has been reported as a new machinable biomaterial, and might be used in dental and orthopedic prostheses [17–19].

Forsterite is analogous with enstatite in components, therefore, it is reasonable to assume that forsterite might be biocompatible, possess good mechanical properties, and be useful as a biomaterial. The objective of this work is to synthesize pure forsterite powder, fabricate forsterite ceramics and study their sinterability, microstructure and mechanical properties. In addition, the in vitro behavior of osteoblasts on the surface of forsterite ceramic was investigated to evaluate its biocompatibility.

2. Materials and methods

2.1. Synthesis of forsterite powders

Forsterite (Mg_2SiO_4) powders were prepared by a sol–gel method using reagent-grade magnesium nitrate hexahydrate ($Mg(NO_3)_2{\cdot}6H_2O$) and colloidal SiO_2 as precursors with an initial MgO to SiO_2 molar ratio of 2. The materials were mixed under vigorous stirring at room temperature for 3 h, then the

* Corresponding author. Tel.: +86 21 52412804; fax: +86 21 52413122.
E-mail address: jchang@mail.sic.ac.cn (J. Chang).

0272-8842/$30.00
doi:10.1016/j.ceramint.2005.07.021

opalescent mixture was aged for 24 h and placed into a 60 °C drying oven overnight to promote gelation. The wet gel was subsequently dried at 120 °C for 48 h. The obtained dry gel was milled for 24 h and sieved to 300-mesh, followed by calcining at different temperatures between 1100 and 1300 °C for 3 h. The calcined powders were analyzed by X-ray diffraction (XRD; Geigerflex, Rigaku, Japan) using monochromated Cu Ka radiation and scanning electronic microscopy (SEM; JSE-6700F, JEOL, Japan).

2.2. Preparation of forsterite ceramics

The synthesized powders were uniaxially pressed at 10 MPa to form a rectangular compact (45.5 mm × 8.0 mm × 3.5 mm) using 6% polyvinyl alcohol (PVA-124) as a binder, then followed by a cold isostatic pressing at 200 MPa. The green samples were subsequently sintered in air at temperatures ranging from 1350 to 1550 °C with a heating rate of 2 °C/min and then furnace cooled. For cell culture tests, disc-shaped pellets 6-mm in diameter and 1.5-mm in thickness were prepared at the same preparation condition.

2.3. Characterization of forsterite ceramics

The phase composition of the sintered specimens was characterized using XRD analysis. The bulk density of the specimens was measured by the Archimedes principle according to ASTM C-20. These were then compared with the theoretical density to obtain relative density. The linear shrinkage of forsterite ceramics was calculated from the length of samples before and after sintering.

For microstructure observation, ceramic bars sintered at 1450 °C were finely polished with a paste containing fine diamond particles smaller than 1.5 μm, then annealed at 1200 °C for 1 h. The 3-point bending strength was measured with a mechanical testing machine (AG-5kNL, Shimadzu Co, Japan) at a crosshead speed of 0.5 mm/min with span length of 30 mm according to the JIS R1601 standard. The single edge precracked bending method was used for the fracture toughness measurement. Sintered samples were ground and notched 3.0 mm deep with a 0.1 mm thick diamond wheel and then evaluated by a material testing machine (Instron 5566, USA). The loading rate was 0.5 mm/min and the span size was 16 mm. In this study, five samples of each group were used to test the average relative density, linear shrinkage and mechanical strength for each condition.

2.4. Culture of osteoblasts on the sintered forsterite ceramics

Osteoblast cells were isolated from calvaria of neonatal (less than 2 days old) Sprague–Dawley rats by an enzymatic digestive process as described previously [20,21]. Briefly, the rat calvaria were washed three times in phosphate-buffered saline (PBS, pH 7.4) and then minced into fragments about 1 mm in diameter. After washing the bone fragments three times with PBS, the chips of calvaria were digested for 20 min at 37 °C with 0.25% (w/v) trypsin-EDTA solution (Gibco, USA) to diminish fibroblastic contamination. Then the samples were treated with 1 mg/ml collagenase (Sigma) at 37 °C for 90 min to release osteoblasts from the calvaria. The supernatants were centrifuged at 1000 rpm for 10 min, and then suspended in the RPMI 1640 (Roswell Park Memorial Institute 1640) medium (Gibco, USA) containing 15% (v/v) heat-inactivated fetal calf serum with 1% glutamine, 50 UI/ml penicillin/streptomycin, and incubated in a 75 cm^2 flask at 37 °C under a humidified atmosphere consisting of 5% CO_2. Culture media were refreshed every 2 days. The cells used in our study were between second and fourth passages.

Prior to cell seeding, the ceramic discs were ultrasonically degreased, cleaned in 75% ethanol, autoclaved for 30 min at 120 °C, and then placed on the well bottoms of a 48-well plate. Then, osteoblasts were rinsed in PBS, detached with a 0.25% (w/v) trypsin-EDTA solution and counted with a hemocytometer. For cell adhesion experiments, osteoblasts were seeded onto the discs at a density of 2×10^3 cells/cm^2 and cell attachment was determined after incubating the cells for 4 and 24 h. Cell proliferation was evaluated after seeding osteoblasts at a density of 1×10^3 cells/cm^2 and incubated for 1, 3 and 7 days. Changes in the number of viable cells on the ceramics in culture were quantitatively by MTT test [22]. MTT (3-[4,5-dimethy-lthiazol-2-yl]-2,5-diphenyltetrazolium bromide) is a yellow tetrazolium salt, which can be enzymatically converted by living cells to a purple formazan product. The intensity of the color produced is therefore directly proportional to the number of viable cells in culture, and thus to their proliferation in vitro. The absorbance of the color observed can be measured at 590 nm (A590). In brief, cells were incubated in an MTT solution at 37 °C for 4 h. After removal of the supernatants, dimethyl sulfoxide (DMSO) was added to each well to completely dissolve the purple formazan. The optical density (OD) of each well was measured at 590 nm in a microplater reader (Elx 800, Bio-Tek, USA). Tissue culture plate served as controls. Five specimens for each material were tested for each incubation time and each test was performed in triplicate. Results were reported as optical density units.

For optical morphological examination, the discs were removed and rinsed twice with PBS to eliminate cells that did not attach to the material. Adhering cells were fixed with methanol for 10 min, washed with PBS and stained with a Giemsa staining solution for 10 min. Discs were then washed with distilled water twice and air-dried. Cellular morphology was observed using inverted phase-contrast microscope (Leica S6D, Germany). For SEM observation, samples were washed with PBS solution twice and fixed in 2.5% glutaraldehyde in 0.1 M sodium-phosphate-buffered solutions for 30 min. This was followed by washing with PBS solution three times and dehydrating in ascending concentrations of ethanol (50, 70, 90, 95 and 100%) for 10 min each. The specimens were then washed with hexamethyldisilazane (HMDS) for 10 min and placed in a desiccator overnight [23]. The dried specimens were glued onto copper specimen stubs, sputter-coated with gold and viewed under SEM.

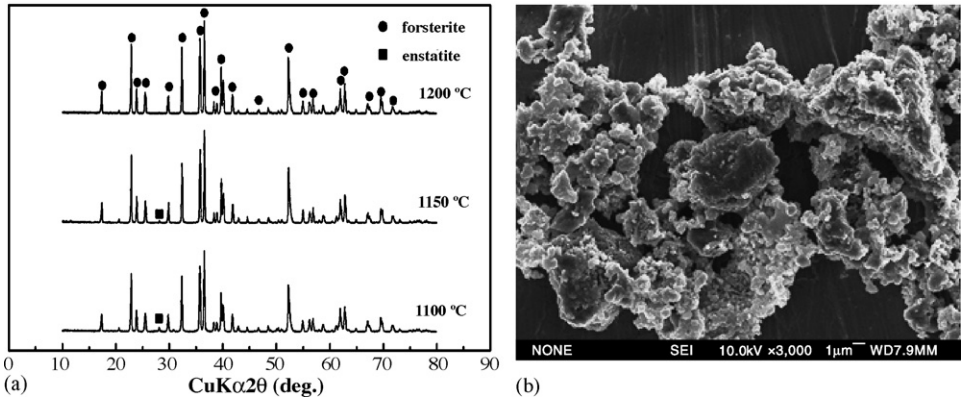

Fig. 1. XRD patterns of forsterite powders heated at temperatures of 1100–1200 °C for 3 h (a) and SEM micrograph of forsterite powders calcined at 1200 °C for 3 h (b).

2.5. Statistical analysis

Statistical analysis was done using Student's *t*-test. All results were expressed as mean ± standard deviation from the quintuple samples in each experiment. Differences were considered statistically significant at $p < 0.05$.

3. Results and discussion

3.1. Characterization of forsterite powders

The XRD patterns displayed the formation of fosterite obtained by calcining at different temperatures. The obvious sharp peaks and low backgrounds suggest that the powders were highly crystalline (Fig. 1a). When the calcination temperature was below 1200 °C, the XRD analysis showed that a small amount of enstatite was formed. As the firing temperature was increased to 1200 °C, all the peaks characterizing the forsterite phase were detected (PDF #80.0783). No peaks characterizing any other phase were detected. The results indicated complete reaction at 1200 °C for 3 h to form stoichiometric forsterite. The morphologies of the forsterite powders fired at 1200 °C shown in Fig. 1b indicated that particles about 5–50 μm agglomerated. The above results indicated that pure forsterite powders were synthesized by a sol–gel method. Increased firing temperature resulted in the improvement of the purity of the prepared powders, i.e. the formation of single-phase forsterite.

3.2. Characterization of forsterite ceramics

The phase composition of the specimens sintered at 1450 and 1550 °C was characterized by means of XRD. The peaks clearly showed only the typical pattern of forsterite (Fig. 2a). The surface microstructure of forsterite sintered at 1450 °C is demonstrated in Fig. 2b. It showed that the average grain size of fosterite was about 10 μm and some small grains about 1–2 μm in grain boundary were also observed. Furthermore, it is clear to see that forsterite powders were sintered apparently with some irregular micropores in powder aggregates and agglomerates, which indicated that the sintered forsterite did not form a dense body.

The sintering behavior and mechanical properties of specimens sintered at different conditions are presented in Tables 1 and 2. Table 1 summarizes the values of the relative density, linear shrinkage, bending strength and fracture toughness variations with changes in sintering temperatures. The linear shrinkage of the sintered forsterite ceramics was apparently influenced by the sintering temperature, which displayed a steady increase from 7.0 to 10.1% with an increase of sintering temperature from 1350 to 1550 °C, and the relative density increased from 82.6 to 91.4% when the sintering temperature varied from 1350 to 1550 °C. In addition, the

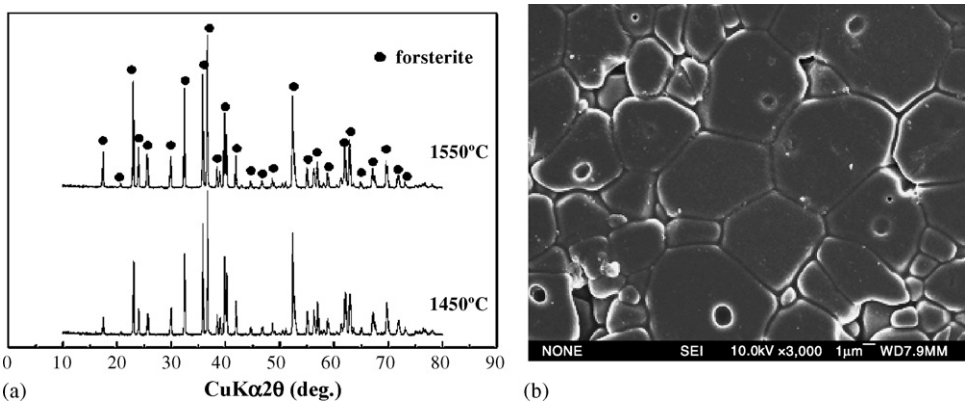

Fig. 2. XRD patterns of forsterite ceramics sintered at 1450 and 1550 °C for 8 h (a) and SEM micrograph of the sintered forsterite ceramics surface at 1450 °C for 8 h (b).

Table 1
Mechanical properties of the fired bodies sintered at different temperature for 6 h

Sintering temperature (°C)	Relative density (%)	Shrinkage (%)	Bending strength (MPa)	Fracture toughness (MPa $m^{1/2}$)
1350	82.6 ± 1.0	7.0 ± 0.2	150 ± 8	1.8 ± 0.4
1450	87.7 ± 1.0	9.0 ± 0.2	181 ± 9	2.3 ± 0.1
1550	91.4 ± 0.6	10.1 ± 0.4	145 ± 8	1.6 ± 0.2

Table 2
Mechanical properties of the fired bodies sintered at different holding times at 1450 °C

Sintering time (h)	Relative density (%)	Shrinkage (%)	Bending strength (MPa)	Fracture toughness (MPa $m^{1/2}$)
3	86.6 ± 0.8	8.2 ± 0.2	152 ± 8	2.1 ± 0.0
6	87.7 ± 1.0	9.0 ± 0.2	181 ± 9	2.3 ± 0.1
8	92.5 ± 0.4	9.2 ± 0.1	203 ± 8	2.4 ± 0.0

mechanical strength of forsterite ceramics was enhanced with the increase of sintering temperature up to 1450 °C. The values of bending strength and fracture toughness reached 181 MPa and 2.3 MPa $m^{1/2}$, respectively. Then, the mechanical strength exhibited a rapid decrease with the increase of sintering temperature to 1550 °C. In general, the density and grain size of ceramics significantly affects the mechanical properties [24,25]. High sintering temperatures often result in extreme grain coarsening and flaw structure. This was evidenced in the fractography, where the fracture surface of the forsterite ceramics sintered at 1450 and 1550 °C showed significant difference. The specimen sintered at 1450 °C had an average grain size of about 10 μm with sharp edged pores which were observed mainly between the grains (Fig. 3a). In contrast, increase in sintering temperature up to 1550 °C caused the pores to be trapped in the grains as a result of grain growth (Fig. 3b), which explained the mechanical properties decrease of the ceramics sintered at 1550 °C. Thus, to get better strength, the optimum sintering temperature of specimen was about 1450 °C.

The holding time was an important factor, which affected the properties of the sintered fosterite ceramics. Table 2 showed the effect of the holding time on relative density, linear shrinkage, bending strength and fracture toughness of the samples sintered at 1450 °C. The samples shrunk increasingly from 8.2 to 9.2% with the increase of holding time from 3 to 8 h. The trend in relative density and fracture toughness was very similar to the pattern encountered with linear shrinkage. It exhibited a gradual increase with increasing holding time. However, the bending strength was sensitive to the holding time and displayed a sharp increase from 152 to 203 MPa with an increase of holding time from 3 to 8 h. Experimental results showed that mechanical strength increased continuously with an increase of sintering time at 1450 °C, in relation with the gain on densification.

Goeuriot et al. have studied the properties of enstatite ($MgSiO_3$) based ceramics from talcs. Their results showed that the enstatite presented higher fracture toughness (2.4 MPa $m^{1/2}$). Although enstatite ceramics possess good mechanical properties, because there are four different polymorphs of enstatite they are unstable and parameters of the fabrication process should be strictly controlled. That is the changes from one form to another depend on temperature, pressure, internal stress in grains and grain size, etc. The destruction effect of phase transformation is caused by the difference in volumes of their grains. The intrinsic stress resulting from the volume changes lead to the loss of mechanical properties [26–28]. In comparison to enstatite, our results showed that the mechanical strength of forsterite was similar to that of enstatite. In addition, no detrimental phase transformations occur during processing for forsterite. Thus, the mechanical property is easier to manipulate. Compared with calcium phosphate ceramics, such as hydroxyapatite ceramics

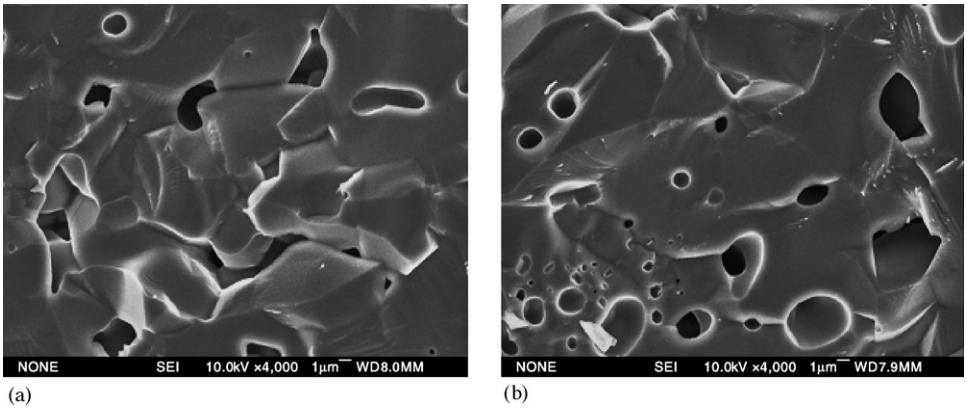

(a) (b)

Fig. 3. SEM of fracture surface of forsterite ceramics after sintering at 1450 °C (a) and 1550 °C (b) for 8 h.

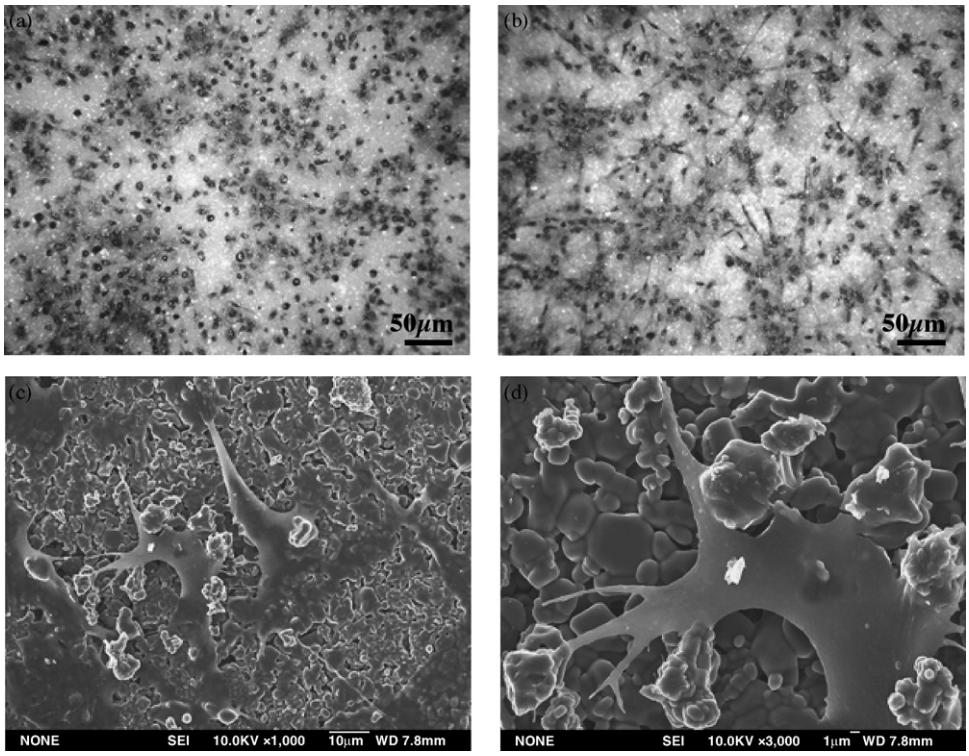

Fig. 4. Phase-contrast microscopic images of rat calvaria osteoblasts cultured on forsterite disks for 4 h (a) and 1 day (b) after seeding. SEM micrographs of forsterite ceramics seeded with osteoblasts and cultured for 1 day (c and d).

(K_{IC} = 0.75–1.2 MPa $m^{1/2}$) [29,30], forsterite ceramics showed a significant improvement in the fracture toughness (K_{IC} = 2.4 MPa $m^{1/2}$), superior to the lower limit reported for cortical bone [4]. In addition, the relative density obtained from forsterite ceramics was only 92.5%, which suggests that a further improvement of the mechanical properties might be obtained by other sintering methods, such as liquid phase sintering, the hot-pressing technique and the spark plasma sintering process [31], which might lead to denser forsterite ceramics.

3.3. Evaluation of biocompatibility of forsterite ceramics

Light and scanning electron microscopy showed the morphological features of osteoblasts cultured on the forsterite ceramics for 4 and 24 h, respectively. It was noted that significant differences in cell shapes were observed at 4 and 24 h. (Fig. 4). At an early stage of culture (4 h after cell seeding), many cells attached to the material surface and mainly presented a spherical or triangular morphology (Fig. 4a). Furthermore, some cells showed initial spreading, as evidenced by small round cells on the ceramics. After 24 h, the attachment and spreading were more obvious. Most of cells adhered tightly to the sample surface and spread with elongated shapes. However, some rounded and less spread out cells could still be observed (Fig. 4b). From high magnification SEM micrographs, it is clear to see the cells presented a close contact with the surface and adopted irregular morphology. Thin cytoplasmic digitations could be observed. Moreover, osteoblasts presented a smoother dorsal surface and plump configuration (Fig. 4c and d). MTT test showed that osteoblasts exhibited a high degree of proliferation. The OD values of cell proliferation on the pure forsterite ceramics and on the control plate are exhibited in Fig. 5, which shows that the degree of cell proliferation on the forsterite apparently increased with the increase of culture time. Forsterite showed a significantly higher proliferation rate when compared with the control over a period of 7 days ($p < 0.05$). The higher proliferation rate of ceramics confirmed that forsterite promoted the proliferation of osteoblasts without a cytotoxic effect. Based on the above results, the forsterite was considered to have good cell biocompatibility. In the previous study, Dubous et al. showed that enstatite ceramics also promoted the proliferation of rat osteoblasts, and osteoblasts adhered better to enstatite than to

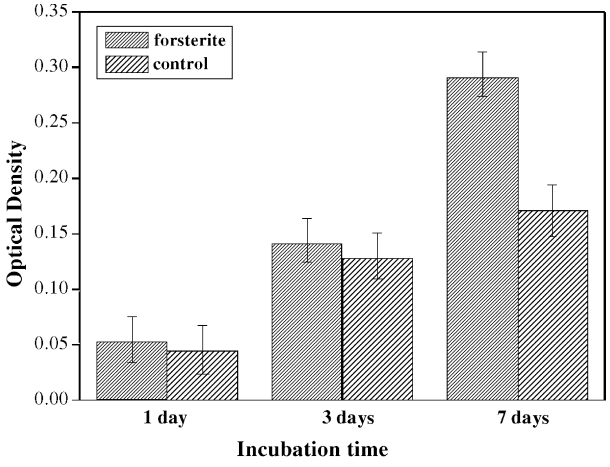

Fig. 5. Proliferation of osteoblasts cultivated on forsterite ceramics for 1, 3 and 7 days in comparison with the control.

Thermanox® or to glass. They explained that the cause of the greater cell viability on enstatite was probably due to its rough, irregular surface topography [17,18]. A rough surface induced a better cell attachment than those presenting smooth surfaces, such as plastic. In our study, we noticed that the surface topography of forsterite also appeared rough, which was probably an important factor to support osteoblast adhesion and proliferation.

4. Conclusions

In this study, pure forsterite ceramics were prepared by sintering forsterite sol–gel derived powder compacts. The behavior of forsterite compacts sintered at different conditions was studied to examine their sintering behaviors and mechanical properties. The results showed that the optimal bending strength (203 MPa) and fracture toughness (2.4 MPa $m^{1/2}$) of forsterite ceramics were higher than that of currently available hydroxyapatite ceramics. The in vitro study showed the significant osteoblasts adhesion, spreading and growing on the surface of forsterite ceramic. In addition, MTT tests demonstrated that the osteoblast proliferation rate was significantly higher on the surface of the sintered forsterite ceramics than on the controls after 7 days ($p < 0.05$). In conclusion, forsterite bioceramics possessed improved mechanical properties and good biocompatibility and might be suitable for hard tissue repair.

Acknowledgment

This work is financially supported by the Science and Technology Commission of Shanghai Municipality under grant no.: 02JC14009.

References

[1] J.N. Kent, J.H. Quinn, M.F. Zide, I.M. Figer, M. Jarcho, S.S. Rothstein, Correction of alveolar ridge deficiencies with non-resorbable hydroxyapatite, J. Am. Dent. Assoc. 105 (1982) 993–1001.
[2] P. Scheer, P.J. Boyne, Maintenance of alveolar bone through implantation of bone graft substitutes in tooth extraction sockets, J. Am. Dent. Assoc. 114 (1987) 594–597.
[3] A. Piatteli, G. Podda, A. Scarano, Clinical and histological results in alveolar ridge enlargement using coralline calcium carbonate, Biomaterials 18 (1997) 623–627.
[4] L.L. Hench, Bioceramics, J. Am. Ceram. Soc. 81 (1998) 1705–1728.
[5] C.C. Mardare, A.I. Mardare, J.R.F. Fernandes, E. Joanni, S.C.A. Pina, M.H.V. Fernandes, R.N. Correia, Deposition of bioactive glass-ceramic thin-films by RF magnetron sputtering, J. Eur. Ceram. Soc. 23 (2003) 1027–1030.
[6] C. Vitale-Brovarone, S. Dinunzio, O. Bretcanu, E. Verne, Macroporous glass-ceramic materials with bioactive properties, J. Mater. Sci. Mater. Med. 15 (2004) 209–217.
[7] T. Kobayashi, K. Okada, T. Kuroda, K. Sato, Osteogenic cell cytotoxicity and biomechanical strength of the new ceramic diopside, J. Biomed. Mater. Res. 37 (1997) 100–107.
[8] C.T. Wu, J. Chang, Synthesis and apatite-formation ability of akermanite, Mater. Lett. 58 (2004) 2415–2417.
[9] H.S. Ryu, K.S. Hong, J.K. Lee, D.J. Kim, J.H. Lee, Magnesia-doped HA/β-TCP ceramics and evaluation of their biocompatibility, Biomaterials 25 (2004) 393–401.
[10] S.R. Kim, J.H. Lee, Y.T. Kim, D.H. Riu, S.J. Jung, Y.J. Lee, S.C. Chung, Y.H. Kim, Synthesis of Si, Mg substituted hydroxyapatites and their sintering behaviors, Biomaterials 24 (2003) 1389–1398.
[11] T.J. Webster, E.A. Massa-Schlueter, J.L. Smith, E.B. Slamovich, Osteoblast response to hydroxyapatite doped with doped with divalent and trivalent cations, Biomaterials 25 (2004) 2111–2121.
[12] E.M. Carlisle, Silicon: a possible factor in bone calcification, Science 167 (1970) 279–280.
[13] K. Schwarz, D.B. Milne, Growth-promoting effects of silicon in rats, Nature 239 (1972) 333–334.
[14] R.Z. LeGeros, Calcium Phosphates in Oral Biology and Medicine, Basel, Switzerland, 1991.
[15] J. Althoff, P. Quint, E.R. Krefting, H.J. Höhling, Morphological studies on the epiphyseal growth plate combined with biochemiacal and X-ray microprobe analyasis, Histochemistry 74 (1982) 541–552.
[16] T. Ban, Y. Ohya, Y. Takahashi, Low-temperature crystallization of forsterite and orthoenstatite, J. Am. Ceram. Soc. 82 (1999) 22–26.
[17] J.C. Dubois, P. Exbrayat, M.L. Couble, D. Goueriot, M. Lissac, Effects of new machinable ceramic on behavior of rat bone cells cultured in vitro, J. Biomed. Mater. Res. 43 (1998) 215–225.
[18] J.C. Dubois, C. Souchier, M.L. Couble, P. Exbrayat, M. Lissac, An image analysis method for the study of cell adhesion to biomaterials, Biomaterials 20 (1999) 1841–1849.
[19] D. Goeuriot, J.C. Dubois, D. Merle, F. Thevenot, P. Exbrayat, Enstatite based ceramics for machinable prosthesis applications, J. Eur. Ceram. Soc. 18 (1998) 2045–2056.
[20] C.G. Bellows, J.E. Aubin, J.N.M. Heersche, M.E. Antosz, Mineralised bone nodules formed in vitro from enzymatically released rat calvaria cell populations, Calcif. Tissue Int. 38 (1986) 143–154.
[21] S.L. Ishaug, M.J. Yaszemski, R. Bizios, A.G. Mikos, Osteoblast function on synthetic biodegradable polymers, J. Biomed. Mater. Res. 28 (1994) 1445–1453.
[22] D. Dufrane, C. Delloye, I.J. Mckay, P.N. De Aza, S. De Aza, Y.J. Schneider, M. Anseau, Indirect cytotoxicity evaluation of pseudowollastonite, J. Mater. Sci. Mater. Med. 14 (2003) 33–38.
[23] Y. Josset, F. Nasrallah, E. Jallot, M. Lorenzato, O. Dufour-Mallet, G. Balossier, D. Laurent-Maquin, Influence of physicochemical reaction of bioactive glass on the behavior and activity of human osteoblasts in vitro, J. Biomed. Mater. Res. 67 (2003) 1205–1218.
[24] J.L. Shi, Thermodynamics and densification kinetics in solid-state sintering of ceramics, J. Mater. Res. 14 (1999) 1398–1408.
[25] R.W. Rice, Grain size and porosity dependence of ceramic fracture energy and toughness at 22 °C, J. Mater. Sci. 31 (1996) 1969–1983.
[26] W. Mielcarek, D. Nowak-Woźny, K. Prociów, Correlation between $MgSiO_3$ phases and steatite ceramics mechanical durability, J. Eur. Ceram. Soc. 24 (2004) 3817–3821.
[27] W.E. Lee, A.H. Heuer, On the polymorphism of enstatite, J. Am. Ceram. Soc. 70 (1987) 349–360.
[28] J.F. Sarver, F.A. Hummel, Stability relations of magnesium metasilicate polymorphs, J. Am. Ceram. Soc. 55 (1962) 152–156.
[29] M.B. Thomas, R.H. Doremus, Fracture strength of dense hydroxyapatite, Am. Ceram. Soc. Bull. 60 (1981) 258–259.
[30] M. Knepper, S. Moricca, B.K. Milthorpe, Stability of hydroxyapatite while processing short-fibre reinforced hydroxyapatite ceramics, Biomaterials 18 (1997) 1523–1529.
[31] Z. Shen, E. Adolfsson, M. Nygren, L. Gao, H. Kawaoka, K. Niihara, Dense hydroxyapatite-zirconia ceramic composites with high strength for biological application, Adv. Mater. 13 (2001) 214–216.